The following publication X. You, Z. Liu, M. Gao, J. Chen, C. Yu, and G. Shen, "Indoor Three-Dimensional Optical Wireless Positioning and Orienteering Using Steerable Line Lasers," in Asia Communications and Photonics Conference/International Conference on Information Photonics and Optical Communications 2020 (ACP/IPOC), K. Xu, D. Simeonidou, C. Chang-Hasnain, N. Wada, X. Ren, Z. Zhukov, P. Perry Shum, Y. Ji, J. Zhang, X. Zhou, C. Lu, and L. Wosinska, eds., OSA Technical Digest (Optica Publishing Group, 2020), paper M4A.226 is available at https://doi.org/10.1364/ACPC.2020.M4A.226.

Indoor Three-Dimensional Optical Wireless Positioning and Orienteering Using Steerable Line Lasers

Xiaodi You[1], Zhongxu Liu[2], Mingyi Gao[1], Jian Chen[3], Changyuan Yu[2], Gangxiang Shen[1,*]
[1] *School of Electronic and Information Engineering, Soochow University, Suzhou, China;*
[2] *Department of Electronic and Information Engineering, The Hong Kong Polytechnic University, Hong Kong, China;*
[3] *School of Telecommunications and Information Engineering, Nanjing University of Posts and Telecommunications, Nanjing, China;*
**Corresponding e-mail address: shengx@suda.edu.cn*

Abstract: A 3D optical wireless positioning (OWP) scheme is proposed by observing steering angles emitted from two line lasers with a pair of photo-detectors. OWP accuracy < 10 cm is achieved while offering terminal orientation information.

1. Introduction

Indoor OWP techniques have experienced a vigorous development, serving a variety of location-based services [1]. Proximity based OWP methods are the simplest to implement, but their positioning error is unsatisfied for high-precision applications [2]. To achieve positioning accuracy up to centimeter level, received signal strength (RSS) based trilateration schemes are widely adopted [3]. However, acquisition of RSS usually relies on the ideal emission property of LED luminaires, e.g., the Lambertian model. This adds to complexity for OWP deployment in various indoor spaces. Meanwhile, to enable trilateration, at least three LEDs are required, which limits the use of OWP when there are insufficient LEDs. By using a steerable laser, a ray-surface 3D positioning scheme was proposed [4]. However, the method still needs a Lambertian LED to decide terminal height. Also, receiver orientation is unachievable due to using only a single photo-detector. In this paper, we propose a 3D OWP scheme with two lasers and a pair of photo-detectors. We aim to decouple OWP from light facilities to improve OWP deployment flexibility when luminaire conditions are restricted. According to geometrical derivation, both accurate 3D positioning at centimeter level and terminal orientation can be obtained without knowing the prior information of LED radiation pattern. Numerical results verify the effectiveness of the OWP scheme from different aspects.

2. Proposed Scheme

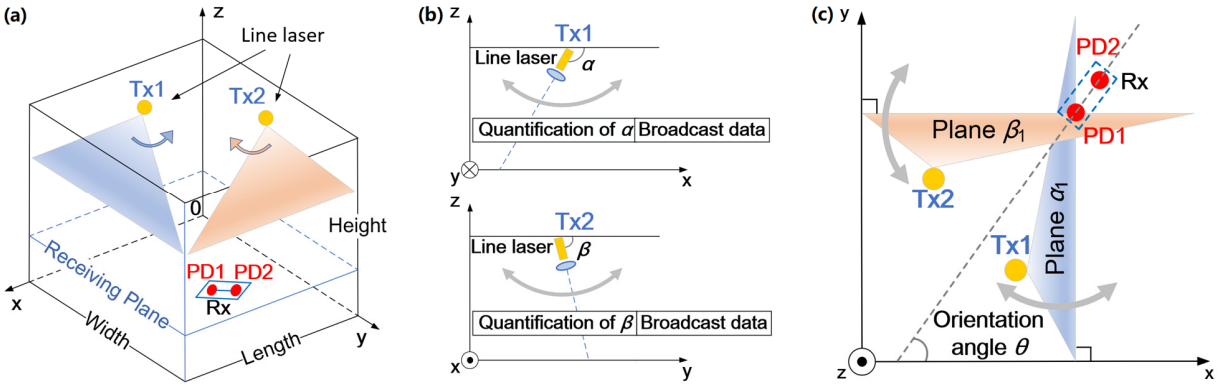

Fig.1. (a) Proposed OWP system; (b) side view; and (c) top view.

As in Fig. 1(a), the proposed OWP system consists of two line lasers as transmitters (Tx1 and Tx2) in the ceiling and a pair of photo-detectors (PD1 and PD2) mounted on the receiver (Rx) terminal in the receiving plane, respectively. Each line lasers can generate a line-shaped beam with a wide fan angle. Examples of line lasers can be found in [5]. Tx1 is located at (x_{t1}, y_{t1}, z_{t1}) and steered along X-axis, and Tx2 is located at (x_{t2}, y_{t2}, z_{t2}) and steered along Y-axis. Tx1 and Tx2 take turns to scan the entire receiving plane rapidly and emit the quantified values of their dynamic steering angles α and β, respectively, as in Fig. 1(b). In this way, signal interference between Tx1 and Tx2 are eliminated so that α and β can be received correctly. Since laser transmitters can be modulated at a high speed, in addition to positioning time slots to convey angular information, we can insert communication time slots to enable indoor data broadcasting. As a result, line-shaped light spots carrying signals from Tx1 and Tx2 will project onto the receiving plane and scan alternately and orthogonally, as in Fig. 1(c).

In the receiving plane, PD1 and PD2 are facing upwards with their coordinates (x_{r1}, y_{r1}, z_{r1}) and (x_{r2}, y_{r2}, z_{r2}), respectively, and their distance is fixed at l. The midpoint between PD1 and PD2 defines the real position of the terminal to be predicted, and the direction pointing from PD2 towards PD1 defines the terminal orientation, i.e., the anticlockwise angular rotation θ with respect to X-axis. By adopting optical filters at PD1 and PD2, encoded angular information from Tx1 and Tx2 can be recovered successfully under normal illumination circumstances. From Fig. 1(c), PD1 can receive angular signal of α_1 and β_1 emitted from Tx1 and Tx2, and PD2 can receive α_2 and β_2 from Tx1 and Tx2, respectively. Let us use N_d bits to quantify both α and β. Thus, both increments $\Delta\alpha$ and $\Delta\beta$ for steering angles are $180°/2^{N_d}$. Take the quantification of α_1 as an example and assume $k = 0, 1, \ldots, 2^{N_d}-1$, if $k\Delta\alpha < \alpha_1 \le (k+1)\Delta\alpha$, then $\alpha_1 = (k+0.5)\Delta\alpha$. Similar quantization steps also apply to α_2, β_1 and β_2. For PD1, when it receives encoded α_1 from Tx1, we can define Plane α_1 which contains three points, i.e., Tx1, PD1 at ($x_{t1}+z_{t1}\cot\alpha_1$, y_{t1}, 0), and the projection of PD1 on X-axis at ($x_{t1}+z_{t1}\cot\alpha_1$, 0, 0). Thus, Plane α_1 is expressed as

$$\left[(-1)/\left(x_{t1}+z_{t1}\cot\alpha_1\right)\right]x+\left[\left(-\cot\alpha_1\right)/\left(x_{t1}+z_{t1}\cot\alpha_1\right)\right]z+1=0. \tag{1}$$

Meanwhile, when PD1 receives β_1 from Tx2, it should be within Plane β_1 which could be described as

$$\left[(-1)/\left(y_{t2}+z_{t2}\cot\beta_1\right)\right]y+\left[\left(-\cot\beta_1\right)/\left(y_{t2}+z_{t2}\cot\beta_1\right)\right]z+1=0. \tag{2}$$

Therefore, PD1 is within the intersection line of Planes α_1 and β_1. Its coordinate is given in the point-slope form

$$\left[\hat{x}_{r1}-\left(x_{t1}+z_{t1}\cot\alpha_1\right)\right]/\left(-\cot\alpha_1\right)=\left[\hat{y}_{r1}-\left(y_{t2}+z_{t2}\cot\beta_1\right)\right]/\left(-\cot\beta_1\right)=\hat{z}_{r1}. \tag{3}$$

Similarly, PD2 also locates within the intersection line of Planes α_2 and β_2, with its coordinate written as

$$\left[\hat{x}_{r1}-\left(x_{t1}+z_{t1}\cot\alpha_2\right)\right]/\left(-\cot\alpha_2\right)=\left[\hat{y}_{r1}-\left(y_{t2}+z_{t2}\cot\beta_2\right)\right]/\left(-\cot\beta_2\right)=\hat{z}_{r1}. \tag{4}$$

Due to the fixed distance l between PD1 and PD2, we have the following constraint condition

$$\left(\hat{x}_{r1}-\hat{x}_{r2}\right)^2+\left(\hat{y}_{r1}-\hat{y}_{r2}\right)^2+\left(\hat{z}_{r1}-\hat{z}_{r2}\right)^2=l^2. \tag{5}$$

Let $\hat{z}_{r1} = \hat{z}_{r2} = h$, after substituting (3) and (4) into (5), the following relationship can be obtained

$$P\left(h-\hat{z}_{t1}\right)^2+Q\left(h-\hat{z}_{t2}\right)^2=l^2, \tag{6}$$

where $P = (\cot\alpha_1-\cot\alpha_2)^2$ and $Q = (\cot\beta_1-\cot\beta_2)^2$. Solving h in (6) will result in two potential solutions

$$h_{1,2}=\left[\left(Pz_{t1}+Qz_{t2}\right)\pm\sqrt{\left(Pz_{t1}+Qz_{t2}\right)^2-\left(P+Q\right)\left(Pz_{t1}{}^2+Qz_{t2}{}^2-l^2\right)}\right]/\left(P+Q\right). \tag{7}$$

Accordingly, by substituting $h_{1,2}$ into (3) and (4), we can get two pairs of coordinates for PD1 and PD2.

To find out the real locations for PD1 and PD2, we first rule out the solution if it is out of the room range considered. Next, we compare the received angular information emitted from Tx1 and Tx2 to make a judgment as follows. Specifically, if $\alpha_1 \le \alpha_2$ and $\beta_1 \le \beta_2$, then we select the coordinate pair with $\hat{x}_{r1} \ge \hat{x}_{r2}$ and $\hat{y}_{r1} \ge \hat{y}_{r2}$; if $\alpha_1 > \alpha_2$ and $\beta_1 \le \beta_2$, then we select the coordinate pair with $\hat{x}_{r1} < \hat{x}_{r2}$ and $\hat{y}_{r1} \ge \hat{y}_{r2}$; if $\alpha_1 \le \alpha_2$ and $\beta_1 > \beta_2$, then we select the coordinate pair with $\hat{x}_{r1} \ge \hat{x}_{r2}$ and $\hat{y}_{r1} < \hat{y}_{r2}$; otherwise, if $\alpha_1 > \alpha_2$ and $\beta_1 > \beta_2$, we select the coordinate pair with $\hat{x}_{r1} < \hat{x}_{r2}$ and $\hat{y}_{r1} < \hat{y}_{r2}$. Finally, the terminal location is calculated as $((\hat{x}_{r1}+\hat{x}_{r2})/2, (\hat{y}_{r1}+\hat{y}_{r2})/2, (\hat{z}_{r1}+\hat{z}_{r2})/2)$. For the terminal orientation angle, if $\hat{y}_{r1} \ge \hat{y}_{r2}$, then $\hat{\theta} = \arccos((\hat{x}_{r1}-\hat{x}_{r2})/l)$; otherwise, if $\hat{y}_{r1} < \hat{y}_{r2}$, $\hat{\theta} = 360°-\arccos((\hat{x}_{r1}-\hat{x}_{r2})/l)$.

3. Results and Discussions

The proposed OWP scheme is evaluated via numerical simulations. The size of indoor space is assumed to be 6 m × 6 m × 3 m (length × width × height). The terminal is randomly orientated and the interval between test points is 0.5 m. The distance between PD1 and PD2 is fixed to be 0.1 m, which is close to the length of a smart phone. Fig. 2(a) shows the top view of 3D positioning results within the receiving plane at the height of 1 m. Here N_d = 11 bits are used to quantify α and β, respectively. The mean positioning error in XY-plane and XYZ-space is 4.32 cm and 5.81 cm, respectively. The mean orientation error is 2.20°. In Fig. 2(b), with a higher resolution to quantify α and β, e.g., N_d = 12, OWP accuracy can be improved with 3D positioning error of 2.27 cm at the height of 1 m. Also, it is observed that at the locations farther from transmitters, positioning errors seem larger. This can be solved by dividing the entire

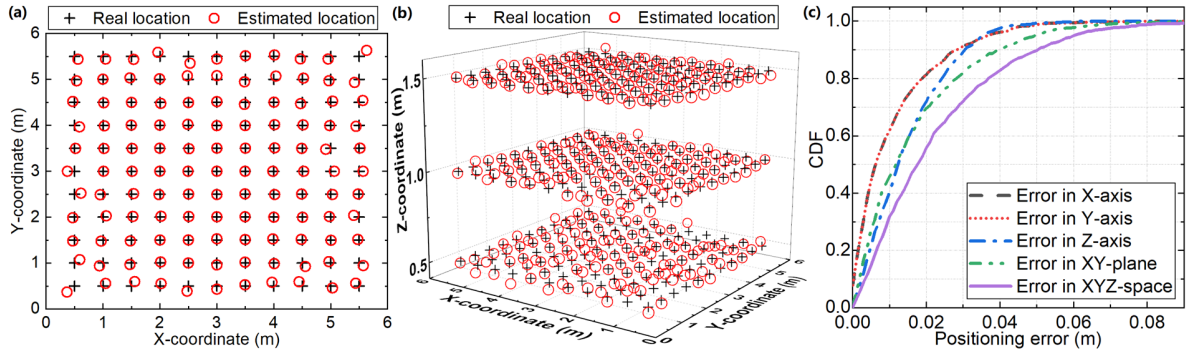

Fig. 2. (a) Top view of 3D positioning results; (b) 3D positioning results; (c) CDF for positioning error. (Tx1: (3, 3, 3); Tx2: (3, 3, 3))

indoor space into subspaces and then deploy each pair of line laser transmitters within each subspace. With N_d = 12, Fig. 2(c) shows the cumulative distribution functions (CDFs) for different types of localization errors within the receiving plane at the height of 1 m. According to statistical results, a total of around 95% 3D positioning errors are less than 6.01 cm, which proves the feasibility of the proposed OWP scheme.

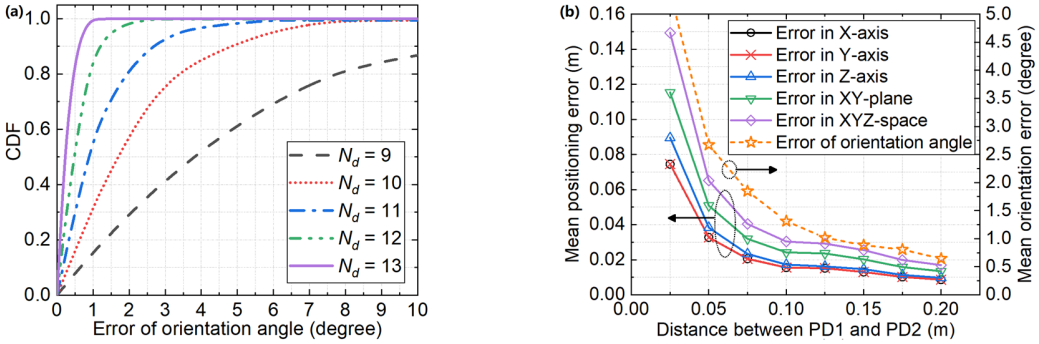

Fig. 3. (a) CDF for orientation error; (b) mean positioning and orientation error. (Tx1: (2, 3, 3); Tx2: (3, 4, 3))

Considering different values of N_d, Fig. 3(a) compares the CDFs for the terminal orientation error. As can be seen, increasing N_d can improve the estimated accuracy of orientation angle effectively. For example, when N_d is 10, 11, 12 and 13, around 90% of orientation errors are less than 4.85°, 2.69°, 1.21° and 0.62°, respectively. It is worth mentioning that terminal devices usually have different sizes. Thus, considering a range of distance l between PD1 and PD2, Fig. 3(b) compares the mean positioning and orientation errors, respectively. When l is as short as 2.5 cm, 3D positioning error is 14.94 cm and orientation error is 5.33° when N_d is 12. However, for a larger device that allows an increasing l, both positioning and orientation errors can be significantly reduced.

4. Conclusions

We propose a 3D positioning and orienteering framework based on optical wireless communication. The geometrical relationship between two line laser transmitters and a pair of receiving photo-detectors are utilized properly. The scheme is simple to implement and features good transplantation, achieving accurate 3D localization at the centimeter level and terminal orientation error < 5° with no need for prior information of lighting luminaires.

5. Acknowledgment

The authors would like to thank the support of Grant 2018YFB1800902 from National Key R&D Program of China.

6. References

[1] J. Luo, L. Fan, and H. Li, "Indoor positioning systems based on visible light communication: state of the art," *IEEE Communications Surveys & Tutorials*, vol. 19, no. 4, pp. 2871-2893, 2017.

[2] G. del Campo-Jimenez, J. M. Perandones, and F. J. Lopez-Hernandez, "A VLC-based beacon location system for mobile applications," in *Proc. IEEE Int. Conf. Localization and GNSS (ICL-GNSS)*, pp. 1-4, 2013.

[3] S. Yang, H. Kim, Y. Son, and S. Han, "Three-dimensional visible light indoor localization using AOA and RSS with multiple optical receivers," *IEEE/OSA Journal of Lightwave Technology*, vol. 32, no. 14, pp. 2480-2485, 2014.

[4] E. W. Lam and T. D. C. Little, "Resolving height uncertainty in indoor visible light positioning using a steerable laser," in *Proc. International Conference on Communications Workshops (ICC Workshops)*, pp. 1-6, 2018.

[5] http://www.cnilaser.com/line_laser.htm.